Thin Solid Films 562 (2014) 467–470

Contents lists available at ScienceDirect

Thin Solid Films

journal homepage: www.elsevier.com/locate/tsf

Control of molecular orientation and morphology in organic bilayer solar cells: Copper phthalocyanine on gold nanodots

Takayuki Sasaki [a], Kenichi Tabata [a], Kazuhito Tsukagoshi [c], Andreas Beckel [d], Axel Lorke [d], Yohei Yamamoto [a,b,*]

[a] Division of Materials Science, Faculty of Pure and Applied Sciences, University of Tsukuba, 1-1-1 Tennodai, Tsukuba, Ibaraki 305-8573, Japan
[b] Tsukuba Research Center for Interdisciplinary Materials Science (TIMS), University of Tsukuba, 1-1-1 Tennodai, Tsukuba, Ibaraki 305-8573, Japan
[c] National Institute for Materials Science, 1-1 Namiki, Tsukuba, Ibaraki 305-0044, Japan
[d] Faculty of Physics, CENIDE, University of Duisburg–Essen, Lotharstraβe 1, Duisburg D-47048, Germany

ARTICLE INFO

Article history:
Received 14 November 2013
Received in revised form 20 March 2014
Accepted 28 March 2014
Available online 4 April 2014

Keywords:
Copper phthalocyanine
C_{60}
Organic photovoltaics
Optical properties
Electronic properties

ABSTRACT

Molecular orientation, morphology of donor (D)/acceptor (A) interface and photoabsorptivity in organic bilayer solar cells were controlled using Au nanodots with an ~20 nm diameter inserted between the bottom electrode and the organic layer. Copper phthalocyanine (CuPc) molecules deposited onto the Au nanodot-coated electrode were mostly oriented face-on with large surface roughness, which is beneficial for photoabsorption, charge separation and transport. Furthermore, Au nanodots exhibit blue-shifted plasmon bands so that CuPc absorbs light more efficiently than that on thin Au layer. Bilayer C_{60}/CuPc solar cells containing Au nanodots exhibited 1.4 times higher photoelectric conversion efficiency than those without Au nanodots. Factors for the enhanced efficiency are (i) improvement of the optical absorption characteristics by face-on orientation of CuPc and (ii) increase of the D/A heterointerface area. In addition, the shift of the plasmon absorption band of Au by the formation of nanodots makes absorption of the CuPc layer much more efficiently, resulting in better photovoltaic output.

1. Introduction

Organic solar cells (OSCs) have recently gained increasing attention due to their advantages, which include reduced weight, mechanical flexibility and cheap and simple fabrication [1]. In particular, organic thin film solar cells have been vigorously developed and power conversion efficiencies (PCEs) as high as 10% were recently achieved [2,3]. In organic thin film solar cells, the interface between electron donor (D) and acceptor (A) molecular layers plays an important role, where a large D/A interface area is required for high charge separation efficiency, leading to better PCE [4–8]. Charge transport and collection properties as well as photoabsorption properties of the organic layers are crucial for the device performance [9–12].

In this study, we investigate the control of the molecular orientation, morphology of the D/A interface and the photoabsorptivity of the organic layer for the purpose of enhancing PCE of bilayer OSCs (Fig. 1a) [13,14]. Copper phthalocyanine (CuPc) and C_{60}-fullerene are used as organic D and A layers, respectively (Fig. 1b). CuPc is known to form a thin film with an edge-on orientation on SiO_2-covered Si, indium-tin-oxide (ITO), and PEDOT:PSS-coated substrate surfaces (PEDOT = poly(3,4-ethylenedioxythiophene), PSS = poly(styrenesulfonate)) [15–17]. However, this edge-on orientation is not appropriate for charge carrier transport in sandwich-type OSCs, since the direction of charge transport is perpendicular to the surface of the substrate. On the other hand, on Au surfaces, CuPc tends to stack with a face-on orientation [18–20], which is better for charge transport in OSCs. Here, we utilize a thin layer of Au between the ITO electrode and the organic layer. For increasing C_{60} (A)/CuPc (D) interface area, we fabricated a dot-like structure of Au with an average diameter (d_{av}) of 18 nm, which is close to the exciton diffusion length (~20 nm). We found that CuPc, deposited on the Au dot-coated ITO electrode, has face-on orientation, and that C_{60}/CuPc bilayer photovoltaic (PV) cells using the Au nanodots exhibit 1.4 times higher PCE values than those without the Au nanodot layer.

2. Experimental details

For the preparation of Au dots, a thin Au layer (2 nm) was deposited onto a flat ITO glass substrate (Geomatec Co. Ltd.). The Au film was annealed at 800 °C for 10 min under an inert atmosphere (0.5 L min^{-1} N_2 gas flow) using an infrared lamp annealer. The resultant Au nanodots were characterized by scanning electron microscopy (SEM, Hitachi model S-4800 field-emission scanning electron microscopy, operation voltage: 10 kV) and atomic force microscopy (AFM, SII-Nanotechnology model S-image scanning probe microscopy). Compounds, CuPc, C_{60} and bathocuproin (BCP) [21,22], were purchased

* Corresponding author. Tel.: +81 29 853 5030; fax: +81 29 853 4490.
E-mail address: yamamoto@ims.tsukuba.ac.jp (Y. Yamamoto).

http://dx.doi.org/10.1016/j.tsf.2014.03.090
0040-6090/

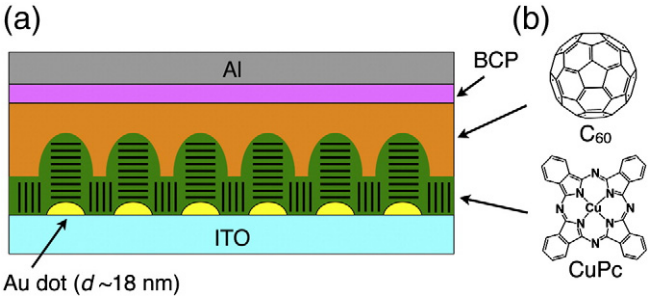

Fig. 1. (a) Schematic representation of the device structure of Al/BCP/C_{60}/CuPc/Au (dots)/ITO photovoltaic cell. (b) Molecular structures of C_{60} and CuPc.

from Aldrich Chemical Co. Ltd. and CuPc was purified twice by thermal sublimation in a reduced pressure ($<5.0 \times 10^{-4}$ Pa). For the fabrication of organic bilayer solar cells, CuPc (20 nm), C_{60} (40 nm) and BCP (10 nm) were subsequently deposited onto an ITO glass substrate (width of ITO electrode line: 2 mm) with and without the Au layer (2-nm-thick film or nanodots). The deposition rate, substrate temperature and background pressure were 0.2 Å s^{-1}, 25 °C and 5.0×10^{-4} Pa, respectively. Then, an Al top electrode (40 nm-thick, 0.5 mm-width) was deposited onto the organic layer. Electronic absorption spectroscopy was measured at 25 °C with a JASCO model V-570 UV/vis/NIR spectrophotometer, where the background absorption by the ITO glass substrate was subtracted. X-ray diffraction (XRD) measurements were performed at 25 °C with a RIGAKU model Miniflex 600 diffractometer (wavelength: 1.5406 Å), equipped with a model D/Tex Ultra2-MF high-speed 1D detector. Photovoltaic properties were evaluated at 25 °C under an atmosphere using a Keithley 4200-SCS semiconductor parameter analyzer, where photoillumination was performed with a SAN-EI model XES-502S solar simulator (AM1.5G, 100 mW cm^{-2}). The light power density was measured using an EKO Instruments model ML-020 silicon photodiode. Dark-field cross-section scanning transmission electron microscopy (XSTEM) was performed with an FEI model Helios NanoLab DualBeam microscope operating at 30 kV and 22 pA. For the sample preparation, an area of 10×5 μm^2 is covered with 3 μm of Pt from a precursor gas. The first 500 nm is deposited by only using the electron beam before turning on the Ga focused ion beam (FIB) to avoid ion implantation. The surrounding material is then removed by milling 10 μm deep trenches using the FIB and the uncovered piece is attached to a micro-manipulator by using FIB Pt deposition. The base is then removed by the FIB and the isolated piece is attached to a copper grid. For XSTEM, the cross-section is thinned using the FIB to about 100 nm. During the thinning, the ion beam current is gradually decreased, which reduces surface roughness and Ga accumulation. The final dimension of the cross-section is about $10 \times 5 \times 0.1$ μm^3.

3. Results and discussion

Fig. 2a shows SEM images of an Au thin layer on an ITO substrate before annealing, displaying that the Au layer consists of fused small dots with d_{av} of 6–8 nm. When annealed at 400 °C, the morphology of the Au film hardly changed. However, as the annealing temperature increased above 600 °C, the dots gradually aggregated, and, after 800 °C annealing, the dot size increased to ~18 nm and each dot became separated (Fig. 2c) [23]. By means of AFM, we determined an increase in the maximum height (h_{max}) by 6.1 nm (12.9 → 19.0 nm; Table 1) after annealing, and a significant increase in the root-mean-square (RMS) roughness of the surface (Table 1, Fig. 2b and d). In addition to the morphological change, the photoabsorption maximum, related to the Au plasmon, blue-shifted from 650 to 550 nm because of the formation of isolated nanodot structures (Fig. 3a, inset) [24,25]. Noteworthy, the ITO electrode was hardly damaged by the short-time annealing at 800 °C, accompanying a slight increase of the resistance (roughly twice).

Fig. 3b shows XRD patterns of these films. The CuPc thin film, deposited directly onto the ITO glass substrate, exhibited a diffraction

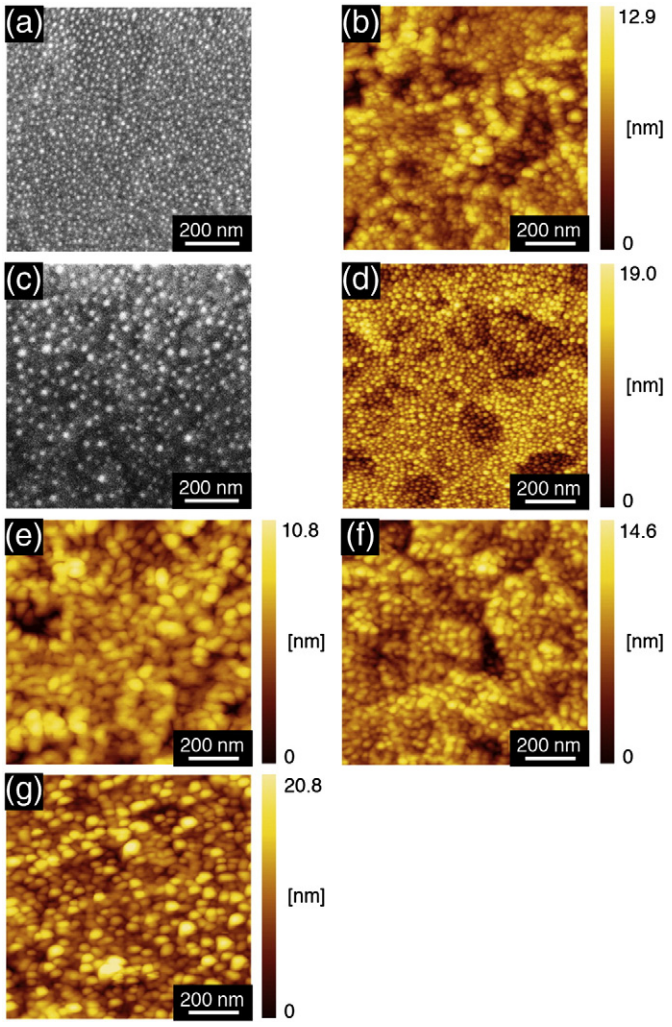

Fig. 2. SEM (a, c) and AFM (b, d) images of Au films (2 nm, a, b) and Au nanodots (c, d) on ITO glass substrates. AFM images of CuPc thin films deposited on ITO (e), Au (film)/ITO (f) and Au (dot)/ITO (g).

maximum at $2\theta = 6.8°$, corresponding to the (200) peak of α-CuPc [26]. This indicates that CuPc aligns with an edge-on orientation. In contrast, the CuPc thin film on Au film displayed significantly smaller diffraction intensity, indicating that CuPc mostly orients in a face-on manner. Furthermore, the intensity of the (200) diffraction for CuPc thin film on Au nanodots is not as strong as for CuPc on ITO, but larger than for CuPc on Au thin film. Therefore, CuPc most likely aligns with a face-on orientation on Au nanodots and with an edge-on orientation on the ITO surface, as depicted in Fig. 1a. According to AFM images, the surface morphology of CuPc thin films on Au dot-coated ITO was clearly different from those on Au thin film or on bare ITO (Fig. 2e–g). For example, h_{max} and RMS roughness of CuPc thin film on ITO (Fig. 2e) were 10.8 and 1.9 nm, respectively, while the corresponding values for CuPc on Au dot-coated ITO (Fig. 2g) were 20.8 and 3.4 nm,

Table 1
Maximum height (h_{max}), average diameter (d_{av}) and RMS roughness of ITO, Au (film)/ITO, Au (dot)/ITO, CuPc/ITO, CuPc/Au (film)/ITO and CuPc/Au (dot)/ITO determined by AFM.

	h_{max} (nm)	d_{av} (nm)	RMS (nm)
ITO	11.7	–	1.8
Au (film)/ITO	12.9	–	1.9
Au (dot)/ITO	19.0	18.0	2.9
CuPc/ITO	10.8	58.1	1.9
CuPc/Au (film)/ITO	14.6	33.7	2.0
CuPc/Au (dot)/ITO	20.8	39.9	3.4

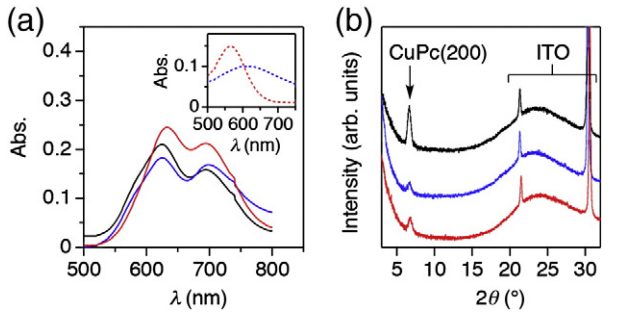

Fig. 3. (a) Electronic photoabsorption spectra of CuPc/ITO (black), CuPc/Au (film)/ITO (blue) and CuPc/Au (dot)/ITO (red). For all spectra, the contributions to the photoabsorption from the ITO glass substrate and the Au (film, dot) were subtracted. Inset shows electronic photoabsorption spectra of a thin Au film (blue) and Au nanodots (red) on ITO glass substrates. (b) XRD patterns of CuPc thin films on ITO (black), Au (film)/ITO (blue) and Au (dot)/ITO (red).

respectively (Table 1). Remarkably, the RMS roughness of the CuPc thin film on Au nanodots (Fig. 2g) was even larger than that of CuPc on Au nanodots (2.9 nm, Table 1 and Fig. 2d). This can be explained by the fact that the face-on oriented CuPc on the Au dots grows faster than the edge-on oriented CuPc on ITO, as schematically depicted in Fig. 1a [10].

The PV properties of the organic bilayer cells (Al/BCP/C_{60}/CuPc/(Au film or dots)/ITO) were investigated. Fig. 4 shows the current density (J)–voltage (V) profiles, where the PV cells with Au nanodots displayed open-circuit voltage (V_{OC}), short-circuit current (J_{SC}), and fill factor (FF) of 0.40 V, 7.2 mA cm^{-2} and 0.38, respectively. The PCE value was 1.10% (Table 2), which was 1.4 times higher than that of the sample prepared on bare ITO (PCE = 0.80%) and 1.5 times higher than that of the sample prepared on a thin Au layer (PCE = 0.74%, Table 2).

We consider that the following two factors contribute to the PCE enhancement in the PV cells with Au nanodots: (i) enhanced photoabsorption properties of CuPc caused by the face-on orientation of CuPc and by an absorption shift of Au accompanied by a formation of nanodots and (ii) increased D/A interface area caused by the surface corrugation. Regarding point (i), the transition dipole moment of CuPc lies in the plane of the molecular disk, therefore the face-on orientation of CuPc will show a higher absorbance than the edge-on orientation. In fact, CuPc on Au nanodot-coated ITO exhibits a larger net absorbance than CuPc on bare ITO (Fig. 3a). On the other hand, the incorporation of Au has a disadvantage, as the Au layer absorbs or reflects light, which reduces the light intensity reaching the organic layer. In this regard, the Au nanodots have an advantage over the continuous Au layer, since the Au nanodots show blue-shifted plasmon bands (650 → 550 nm, Fig. 3a, inset) so that the overlap of the plasmon absorption with the Q-band of CuPc (550–800 nm: Fig. 3a) is reduced. As the result,

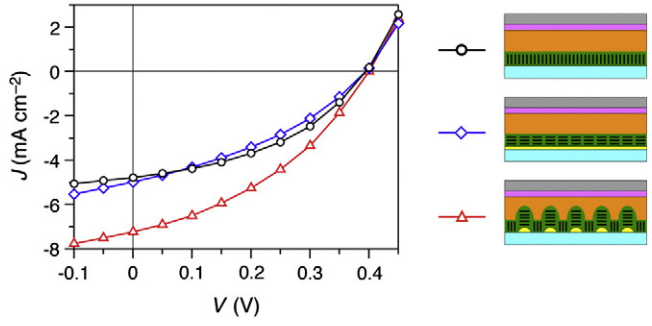

Fig. 4. J–V characteristics of C_{60}/CuPc/ITO (black), C_{60}/CuPc/Au (film)/ITO (blue) and C_{60}/CuPc/Au (dot)/ITO (red) photovoltaic cells under illumination with an AM1.5G solar simulator.

Table 2
V_{OC}, I_{SC}, FF and PCE of PV cells consisting of C_{60}/CuPc/ITO, C_{60}/CuPc/Au (film)/ITO and C_{60}/CuPc/Au (dot)/ITO upon illumination with an AM1.5G (100 mW cm^{-2}) solar simulator.

	V_{OC} (V)	J_{SC} (mA cm^{-2})	FF	PCE (%)
C_{60}/CuPc/ITO	0.39	4.8	0.43	0.80
C_{60}/CuPc/Au (film)/ITO	0.39	5.0	0.38	0.74
C_{60}/CuPc/Au (dot)/ITO	0.40	7.2	0.38	1.10

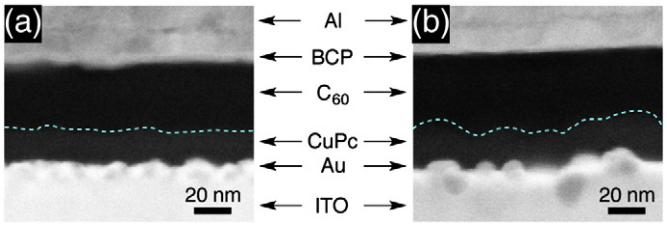

Fig. 5. Dark-field XSTEM images of the C_{60}/CuPc bilayer PV devices on Au (film)/ITO (a) and Au (dot)/ITO (b). The broken lines indicate the interface between C_{60} and CuPc.

J_{SC} of the PV cell using Au nanodot (7.2 mA cm^{-2}) displays the higher values than that without Au dots (4.8 mA cm^{-2}) and even with Au film (5.0 mA cm^{-2}). Regarding point (ii), the RMS roughness of the CuPc layer is 1.8 times increased by inserting the Au nanodot layer (1.9 → 3.4 nm, Table 1), which results in an increase of D/A interface area. As a consequence, excitons can readily reach the D/A interface, leading to an enhancement of the charge separation efficiency. XSTEM experiments show that the C_{60}/CuPc interface is more corrugated in the cell with Au nanodots (Fig. 5b) than in that with Au film (Fig. 5a). On the other hand, FF is reduced when the Au layer (film or dot) is inserted between CuPc layer and ITO electrode (0.43 → 0.38). We initially anticipated that the face-on orientation of CuPc might enhance the charge transport properties in CuPc layer [27], which will lead to the better FF values. It is likely that the charge collection properties become worse when an Au layer is inserted between CuPc layer and ITO electrode. Overall, these factors contribute to the increase of the total PCE for PV cells with an inserted Au nanodot layer. Note that the effect of charge separation by a strong electric field generated by the surface plasmon of the Au dots [28–32] is likely small because, in bilayer PV cells, the direction of the enhanced electric field is perpendicular to the stacked direction of the bilayers.

4. Conclusion

We fabricated organic bilayer photovoltaic cells with inserted Au nanodots between the transparent electrode and the organic layer. Due to the well-optimized photoabsorption, donor/acceptor interface and molecular orientation, the photovoltaic device exhibited 1.4 times higher power conversion efficiency than a reference sample without Au dot layer. This study proves the importance of the molecular orientation that influences the absorptivity of the organic layer in organic photovoltaics. Au nanodots are also useful to corrugate and enlarge the donor/acceptor interface, which contribute to the enhancement of charge separation efficiency.

Acknowledgments

This work was partly supported by MEXT/JSPS KAKENHI Grant Numbers 25107507/25708020, Cooperative Research Program of "Network Joint Research Center for Materials and Devices" (No. 2013A13), Asahi Glass Foundation and University of Tsukuba–DAAD partnership program.

References

[1] J. Peet, M.L. Senatore, A.J. Heeger, G.C. Bazan, The role of processing in the fabrication and optimization of plastic solar cells, Adv. Mater. 21 (2009) 1521.
[2] Z. He, C. Zhong, S. Su, M. Xu, H. Wu, Y. Cao, Enhanced power-conversion efficiency in polymer solar cells using an inverted device structure, Nat. Photonics 6 (2012) 591.
[3] J. You, L. Dou, K. Yoshimura, T. Kato, K. Ohya, T. Moriarty, K. Emery, C.-C. Chen, J. Gao, G. Li, Y. Yang, A polymer tandem solar cell with 10.6% power conversion efficiency, Nat. Commun. 4 (2013) 1446.
[4] G. Li, J. Gao, J.C. Hummelen, F. Wudl, A.J. Heeger, Polymer photovoltaic calls: enhanced efficiencies via a network of internal donor–acceptor heterojunctions, Science 270 (1995) 1789.
[5] F. Yang, S.R. Forrest, Photocurrent generation in nanostructured organic solar cells, ACS Nano 2 (2008) 1022.
[6] Y. Matsuo, Y. Sato, T. Niinomi, I. Soga, H. Tanaka, E. Nakamura, Columnar structure in bulk heterojunction in solution-processable three-layered p-i-n organic photovoltaic devices using tetrabenzoporphyrin precursor and silylmethyl[60]fullerene, J. Am. Chem. Soc. 131 (2009) 16048.
[7] Y. Yamamoto, G. Zhang, W. Jin, T. Fukushima, N. Ishii, A. Saeki, S. Seki, S. Tagawa, T. Minari, K. Tsukagoshi, T. Aida, Ambipolar-transporting coaxial nanotubes with a tailored molecular graphene–fullerene heterojunction, Proc. Natl. Acad. Sci. U. S. A. 106 (2009) 21051.
[8] Y. Moritomo, K. Yonezawa, M. Ito, H. Kamioka, Y. Yamamoto, T. Fukushima, T. Aida, Interface dependence of charge formation dynamics in hexabenzocoronene–C_{60}, Appl. Phys. Express 5 (2012) 062401.
[9] J.E. Allen, K.G. Yager, H. Hlaing, C.-Y. Nam, B.M. Ocko, C.T. Black, Enhanced charge collection in confined bulk heterojunction organic solar cells, Appl. Phys. Lett. 99 (2011) 163301.
[10] Y. Zhou, T. Taima, T. Miyadera, T. Yamanari, M. Kitamura, K. Nakatsu, Y. Yoshida, Glancing angle deposition of copper iodide nanocrystals for efficient organic photovoltaics, Nano Lett. 12 (2012) 4146.
[11] M. Ichikawa, T. Takeuchi, H.-G. Jeon, Y. Jin, S. Lee, K.-S. Kim, Organic photodiode with high infrared light sensitivity based on tin phthalocyanine/C_{60} bulk heterojunction and optical interference effect, Jpn. J. Appl. Phys. 51 (2012) 034103.
[12] K. Yokoyama, T. Kaji, M. Hiramoto, Double co-deposited layered organic photovoltaic cells with sensitivity from visible to near-infrared regions, Jpn J. Appl. Phys. 52 (2013) (04CR06).
[13] C.W. Tang, Two-layered organic photovoltaic cell, Appl. Phys. Lett. 48 (1986) 183.
[14] M. Hiramoto, H. Fujiwara, M. Yokoyama, Three-layered organic solar cell with a photoactive interlayer of codeposited pigments, Appl. Phys. Lett. 58 (1991) 1062.
[15] H. Peisert, X. Liu, D. Olligs, A. Petr, L. Dunsch, T. Schmidt, T. Chasse, M. Knupfer, Highly ordered phthalocyanine thin films on a technically relevant polymer substrate, J. Appl. Phys. 96 (2004) 4009.
[16] M. Rusu, J. Gasiorowski, S. Wiesner, N. Meyer, H. Heuken, K. Fostiropoulos, M.Ch Lux-Steiner, Fine tailored interpenetrating donor–acceptor morphology by OVPD for organic solar cells, Thin Solid Films 516 (2008) 7160.
[17] K. Tabata, T. Sasaki, Y. Yamamoto, Magnetic-field-induced enhancement of crystallinity and field-effect mobilities in phthalocyanine thin films, Appl. Phys. Lett. 103 (2013) 043301.
[18] S. Tokito, J. Sakata, Y. Taga, The molecular orientation in copper phthalocyanine thin films deposited on metal film surfaces, Thin Solid Films 256 (1995) 182.
[19] H. Peisert, T. Schwieger, J.M. Auerhammer, M. Knupfer, M.S. Golden, J. Fink, Order on disorder: copper phthalocyanine thin films on technical substrates, J. Appl. Phys. 90 (2001) 466.
[20] H. Peisert, M. Knupfer, T. Schwieger, J.M. Auerhammer, M.S. Golden, J. Fink, Full characterization of the interface between the organic semiconductor copper phthalocyanine and gold, J. Appl. Phys. 91 (2002) 4872.
[21] Z.R. Hong, Z.H. Huang, X.T. Zeng, Utilization of copper phthalocyanine and bathocuproine as an electron transport layer in photovoltaic cells with copper phthalocyanine/buckminsterfullerene heterojunctions: thickness effects on photovoltaic performances, Thin Solid Films 515 (2007) 3019.
[22] S. Wang, T. Sakurai, R. Kuroda, K. Akimoto, Energy band bending induced charge accumulation at fullerene/bathocuproine heterojunction interface, Appl. Phys. Lett. 100 (2012) 243301.
[23] T. Castro, R. Reifenberger, E. Choi, R.P. Andres, Size-dependent melting temperature of individual nanometer-sized metallic clusters, Phys. Rev. B 42 (1990) 8548.
[24] S. Link, M.A. El-Sayed, Spectral properties and relaxation dynamics of surface plasmon electronic oscillations in gold and silver nanodots and sanorods, J. Phys. Chem. B 103 (1999) 8410.
[25] F.J.G. de Abajo, Nonlocal effects in the plasmons of strongly interacting nanoparticles, dimers, and waveguides, J. Phys. Chem. C 112 (2008) 17983.
[26] M.K. Debe, R.J. Poirier, K.K. Kam, Organic-thin-film-induced molecular epitaxy from the vapor phase, Thin Solid Films 197 (1991) 335.
[27] P. Sullivan, T.S. Jones, A.J. Ferguson, S. Heutz, Structural templating as a route to improved photovoltaic performance in copper phthalocyanine/fullerene (C_{60}) heterojunctions, Appl. Phys. Lett. 91 (2007) 233144.
[28] J.H. Lee, J.H. Park, J.S. Kim, D.Y. Lee, K. Cho, High efficiency polymer solar cells with wet deposited plasmonic gold nanodots, Org. Electron. 10 (2009) 416.
[29] F.-C. Chen, J.-L. Wu, C.-L. Lee, Y. Hong, C.-H. Kuo, M.H. Huang, Plasmonic-enhanced polymer photovoltaic devices incorporating solution-processable metal nanoparticles, Appl. Phys. Lett. 95 (2009) 013305.
[30] J.-L. Wu, F.-C. Chen, Y.-S. Hsiao, F.-C. Chien, P. Chen, C.-H. Kuo, M.H. Huang, C.-S. Hsu, Surface plasmonic effects of metallic nanoparticles on the performance of polymer bulk heterojunction solar cells, ACS Nano 5 (2011) 959.
[31] X. Li, W.C.H. Choy, H. Lu, W.E.I. Sha, A.H.P. Ho, Efficiency enhancement of organic solar cells by using shape-dependent broadband plasmonic absorption in metallic nanoparticles, Adv. Funct. Mater. 23 (2013) 2728.
[32] S.-W. Baek, J. Noh, C.-H. Lee, B.S. Kim, M.-K. Seo, J.-Y. Lee, Plasmonic forward scattering effect in organic solar cells: a powerful optical engineering method, Sci. Rep. 3 (2013) 1726